Lowering an ER stress-regulated long noncoding RNA protects mice from diabetes and isolated pancreatic islets from cell death

Mitsuo Kato,[1,4] Maryam Abdollahi,[1,4] Keiko Omori,[2] Vajir Malek,[1] Linda Lanting,[1] Fouad Kandeel,[2] Jeffrey Rawson,[2] Walter Tsark,[3] Lingxiao Zhang,[1] Mei Wang,[1] Ragadeepthi Tunduguru,[1] and Rama Natarajan[1]

[1]Department of Diabetes Complications and Metabolism, Arthur Riggs Diabetes & Metabolism Research Institute, Beckman Research Institute of City of Hope, 1500 E. Duarte Road, Duarte, CA 91010, USA; [2]Department of Translational Research & Cellular Therapeutics, Arthur Riggs Diabetes & Metabolism Research Institute of City of Hope, 1500 E. Duarte Road, Duarte, CA 91010, USA; [3]Transgenic Mouse Facility, Center for Comparative Medicine, Beckman Research Institute of City of Hope, 1500 E. Duarte Road, Duarte, CA 91010, USA

We investigated the role of the endoplasmic reticulum (ER) stress-regulated long noncoding RNA (lncRNA) lncMGC in pancreatic islets and the pathology of type 1 diabetes (T1D), as well as the potential of lncMGC-based therapeutics. *In vivo*, blood glucose levels (BGLs) and HbA1c were significantly lower in lncMGC-knockout (KO)-streptozotocin (STZ)-treated diabetic mice compared to wild-type STZ. Antisense oligonucleotides (GapmeR) targeting lncMGC significantly attenuated insulitis and BGLs in T1D NOD mice compared to GapmeR-negative control (NC). GapmeR-injected T1D Akita mice showed significantly lower BGLs compared to Akita-NC mice. hlncMGC-GapmeR lowered BGLs in partially humanized lncMGC (hlncMGC)-STZ mice compared to NC-injected mice. CHOP (ER stress regulating transcription factor) and lncMGC were upregulated in islets from diabetic mice but not in lncMGC-KO and GapmeR-injected diabetic mice, suggesting ER stress involvement. *In vitro*, hlncMGC-GapmeR increased the viability of isolated islets from human donors and hlncMGC mice and protected them from cytokine-induced apoptosis. Anti-ER stress and anti-apoptotic genes were upregulated, but pro-apoptotic genes were down-regulated in lncMGC KO mice islets and GapmeR-treated human islets. Taken together, these results show that a GapmeR-targeting lncMGC is effective in ameliorating diabetes in mice and also preserves human and mouse islet viability, implicating clinical translation potential.

INTRODUCTION

Type 1 diabetes (T1D) is the result of pancreas dysfunction leading to insulin secretion deficiency and hyperglycemia and poses a substantial global health challenge.[1] Pancreas β cell loss and dysfunction result from several factors, including autoimmune destruction and insulitis and oxidative and endoplasmic reticulum (ER) stress.[2–8] While exogenous synthetic insulin can preserve life, there is much room for improvement in disease manag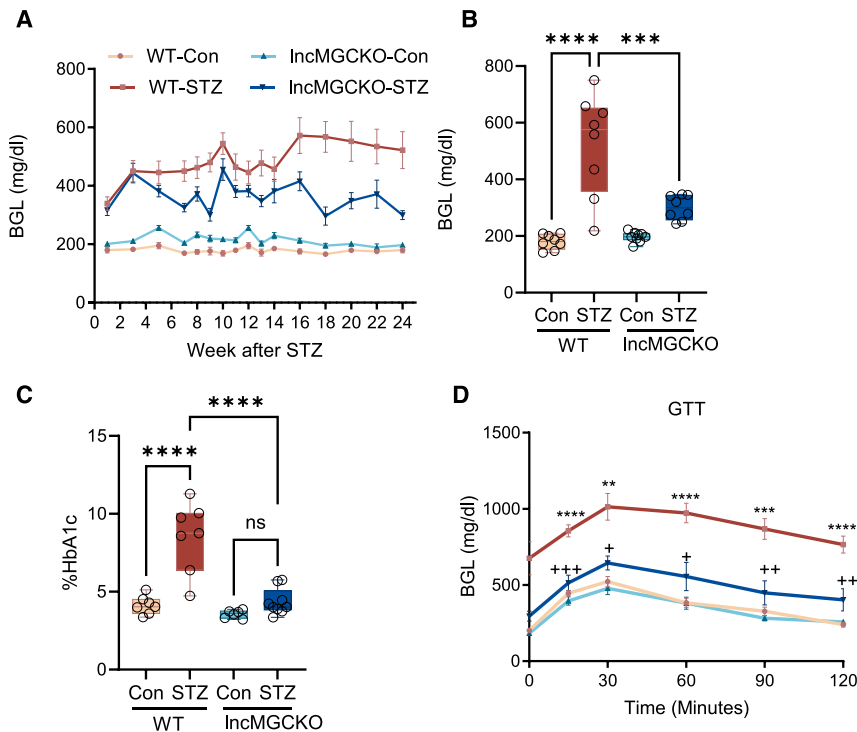ement, especially since T1D is also associated with severe vascular complications such as diabetic kidney disease (DKD).[9–11]

Long noncoding RNAs (lncRNAs) are noncoding transcripts of more than 200 nt and have significant functions in human diseases and gene expression.[12] Notably, various lncRNAs have functions in pancreatic islets and β cells related to diabetes.[13–15] lncRNA MEG3 on chromosome 14q32.2 is posited to be a susceptibility region to T1D.[16] The human lnc-megacluster (lncMGC) lncRNA, which encompasses the miR-379 microRNA (miRNA) cluster of nearly 40 miRNAs from miR-379 (most 5′) to miR-656 (most 3′), is located on human chromosome 14q32.2, while mouse lncMGC, which covers the miR-379 miRNA cluster from miR-379 (most 5′) to miR-3072 (most 3′) is located on mouse chromosome 12qF1.[17,18] Human lncMGC (hlncMGC) shares exons with other lncRNAs such as *MEG8* and *MEG9*[17,19–21] and is significantly elevated in plasma samples from individuals with diabetes and DKD.[22] However, much less is known about the functional roles of lncMGC and ER stress-regulated lncRNAs in pancreatic β cells and T1D, although ER stress modulates β cell survival and T1D development.[3–5,8] lncRNA lncMGC is upregulated via the key ER stress-related transcription factor C/EBP homologous protein (CHOP) in the kidneys of diabetic mice and induced features of early DKD such as hypertrophy and fibrosis.[17] Moreover, genetic deletion of miR-379 (miR-379 knockout [KO] mice) protected diabetic[23] and obese[24] mice from kidney disease through the

Figure 1. lncMGC KO mice exhibit resistance to STZ-driven diabetes

Diabetes was induced by intraperitoneal injections of STZ (50 mg/kg daily for 5 consecutive days) in 10-week-old male mice. (A) Weekly and (B) endpoint BGLs in WT and lncMGC KO Con and diabetic mice, 24 weeks after onset of diabetes. $n = 8$ mice/group. (C) HbA1c (%) levels. $n = 5–7$ mice/group. One-way ANOVA with post hoc Tukey's test for multiple comparisons. ***$p < 0.001$; ****$p < 0.0001$; ns, not statistically significant. (D) GTT at 24 weeks of diabetes. $n = 6$ mice/group. **$p < 0.01$; ***$p < 0.001$; ****$p < 0.0001$ WT-STZ versus WT-Con and $^+p < 0.05$; $^{++}p < 0.01$; $^{+++}p < 0.001$ lncMGC KO-STZ versus WT-STZ, using 2-way repeated-measures ANOVA. Data are presented as mean ± SEM.

A1c (HbA1c, %) levels in lncMGC KO-STZ mice were also lower than those in WT-STZ mice and were similar to control (Con) non-diabetic mice (Figure 1C). Interestingly, lncMGC KO-STZ mice exhibited significantly improved glucose tolerance at 15 min after the challenge compared to WT-STZ mice (Figure 1D), suggesting improved pancreas β cell function in lncMGC KO mice. lncMGC KO mice showed greater pancreata weights compared to WT Con (Figure S1). These data stimulated further inquiry into a putative role of lncMGC in diabetes development.

Pancreata from WT-STZ mice had significantly smaller islets compared to WT-Con mice, whereas lncMGC KO-STZ mice had intact islets that were similar to Con mice (Figure 2A). There was less immunoreactive islet insulin in the pancreas from WT-STZ mice compared to WT-Con mice, as expected. In contrast, insulin was more abundant in islets from lncMGC KO-STZ mice (Figures 2A and 2B). ER stress is an important factor in the pathogenesis of T1D,[3–5,8] and lncMGC is regulated by the ER stress-related transcription factor CHOP.[17] The protein levels of CHOP were measured using immunohistochemical (IHC) staining (Figure 2A). CHOP expression was significantly higher in WT-STZ islets compared to WT-Con islets (Figures 2A and 2C). Notably, this increase was significantly reduced in lncMGC KO-STZ mice, with levels similar to Con islets (Figures 2A and 2C). As expected, lncMGC RNA expression was absent in islets isolated from lncMGC KO mice (Figure 2D). In addition, decreased miR-379 was also confirmed in lncMGC KO islets (Figure 2E). Interestingly, anti-ER stress (*Edem3*, target of miR-379)[17,25] and anti-apoptotic (*Bcl2*) genes were upregulated, but pro-apoptotic genes (*Puma, Bad, Bid, Bim*)[26] were downregulated in lncMGC KO islets. Mitophagy-related gene *Fis1* (target of miR-379)[23] was also increased in lncMGC KO islets (Figure 2E), suggesting that changes in such ER stress, mitophagy,[27,28] and mitophagy-regulated apoptotic genes might support resistance to STZ-induced diabetes in lncMGC KO mice.

reduction of ER stress and/or improved mitophagy.[23] Additionally, KO mice lacking CHOP were protected from DKD through the reduction of lncMGC, miR-379 cluster miRNAs, and CHOP.[17] An inhibitor of lncMGC, GapmeR (locked nucleic acid [LNA] and phosphorothioate-modified antisense oligonucleotide) was found to efficiently inhibit expression of the miR-379 cluster miRNAs and lncMGC, and also features of early DKD (including fibrosis) in mice.[17] More recently, we showed that lncMGC, as a nucleosome-remodeling factor-interacting RNA, enhanced specific gene expression related to DKD through chromatin relaxation.[18] However, it is unclear whether ER stress associated with lncMGC upregulation modulates pancreatic islet function and T1D development. In the present study, we tested the hypothesis that suppressing lncMGC in several types of diabetic mice and in human and mouse islets would improve glucose homeostasis and islet viability, at least in part via attenuation of ER stress-related mechanisms.
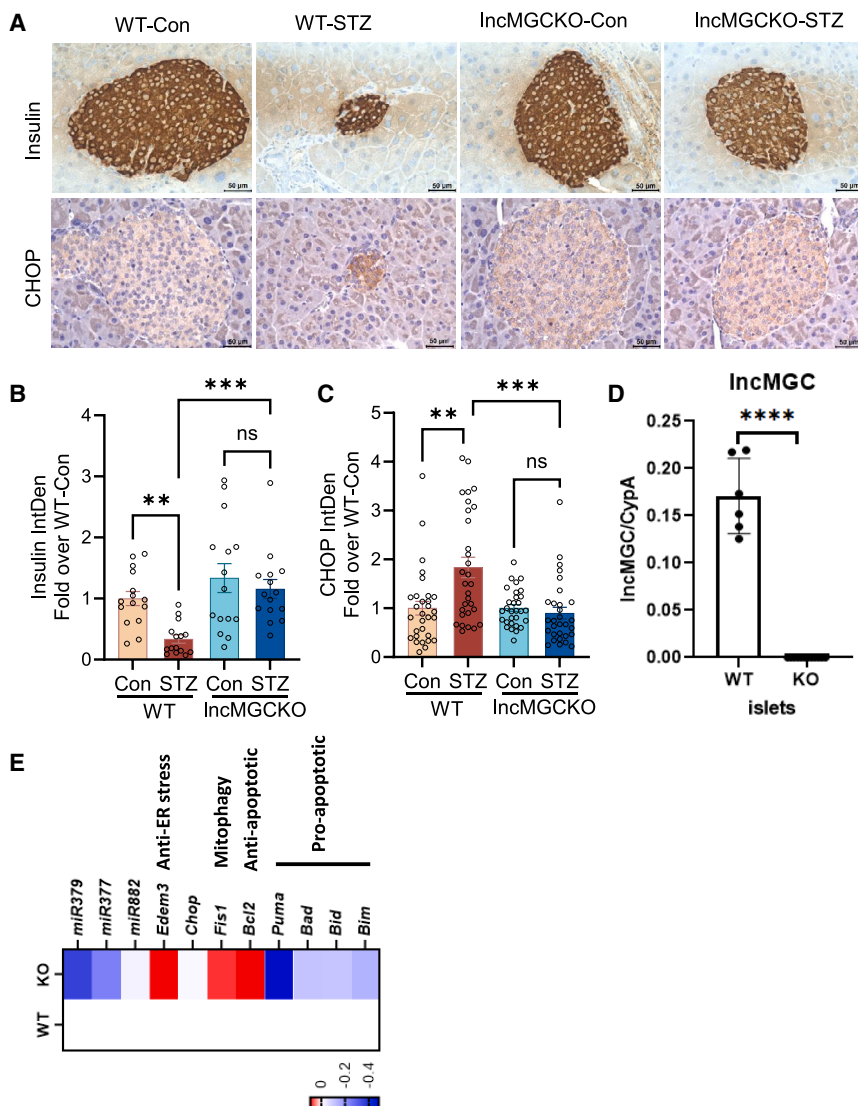
RESULTS

lncMGC KO mice were protected from streptozotocin (STZ)-induced diabetes

Using CRISPR-Cas editing, we generated lncMGC KO mice as described earlier.[18] Several lines of mutants were obtained (including lncMGC KO1 and lncMGC KO5),[18] and lncMGC KO5 was used in the present study.[18] STZ (50 mg/kg/day for 5 days) was used to induce diabetes in lncMGC KO5 mice as described earlier.[23] Blood glucose levels (BGLs) were monitored for 24 weeks (Figures 1A and 1B). lncMGC KO-STZ mice displayed significantly lower BGLs compared to wild-type (WT)-STZ mice at 24 weeks (Figure 1B). Hemoglobin

Figure 2. Pancreas structure, insulin levels, and key functional marker genes in Con and diabetic lncMGC KO mice

(A) IHC staining of insulin and CHOP (ER stress regulator) in pancreatic islets in WT and lncMGC KO Con and STZ mice 24 weeks after onset of diabetes. Scale bar, 50 μm. 40× magnification. (B and C) Quantitative analysis, IntDen, of (B) insulin ($n = 15$ islet/group) and (C) CHOP ($n = 30$ islet/group). (D) lncMGC RNA expression in isolated islets from WT and lncMGC KO Con mice. (E) Heatmap shows expression of miR-379; miR-377 (key miRNAs within the lncMGC miRNA cluster); miR-882 (which is located outside of miR-379 cluster); *Edem3,* an anti-ER stress marker; *Chop*, an ER stress marker; *Bcl2* (anti-apoptotic); *Puma*, *Bad*, *Bid*, *Bim* (pro-apoptotic genes); and *Fis1* (mitophagy-related gene) in isolated islets from WT and lncMGC KO Con male mice. $n = 6$ mice/group. Kruskal-Wallis test with Dunn's multiple comparisons test. Statistical comparisons between 2 groups were performed using 2-sided Student's t test. **$p < 0.01$; ***$p < 0.001$; ****$p < 0.0001$; ns, not statistically significant. Data are presented as mean ± SEM.

of nucleotide sequence.[17] Using CRISPR-Cas9 editing, we created partially humanized mice by replacing the mouse lncMGC sequences with hlncMGC sequences, as detailed in the Materials and methods section (Figure S3). PCR with human-specific primers confirmed the replacement of the human sequence in the hlncMGC mice (H/H in Figure S3). Initially, diabetes was induced in miR-379KO mice[23] with two regimens of STZ dosing (40 mg/kg/day for 4 days or 50 mg/kg/day for 5 days) to optimize the best condition for STZ treatment in the hlncMGC mice. miR-379KO mice had heavier pancreata compared to WT mice (Figure S4A). Data from miR-379KO mice (Figure S4B) showing protection from diabetes supported the use of the lower amount of STZ (40 mg/kg/day for 4 days, inducing milder diabetes) for subsequent studies in the hlncMGC mice. Diabetic hlncMGC mice were injected subcutaneously with a GapmeR-NC or the GapmeR-targeting hlncMGC (GapmeR [HMGC10]) (5 mg/kg weekly for 4 weeks) (Figure 3). GapmeR was injected after the onset of diabetes. Age-matched hlncMGC mice served as Con. Following treatment, the target-specific GapmeR (HMGC10) was found in the pancreas of treated animals (Figure 3A). GapmeR-treated diabetic mice showed significantly lower BGLs (Figures 3B and 3C). Furthermore, after a glucose bolus, GapmeR-treated mice had faster restoration of glucose balance compared to hlncMGC STZ/NC, suggesting improvement in β cell function (Figures 3D and 3E). IHC staining revealed more islet insulin in the hlncMGC STZ/Gap mice (Figures 4A and 4B). GapmeR treatment of hlncMGC STZ mice was also associated with increased size and number of pancreatic islets (Figures 4A and 4C). In addition,
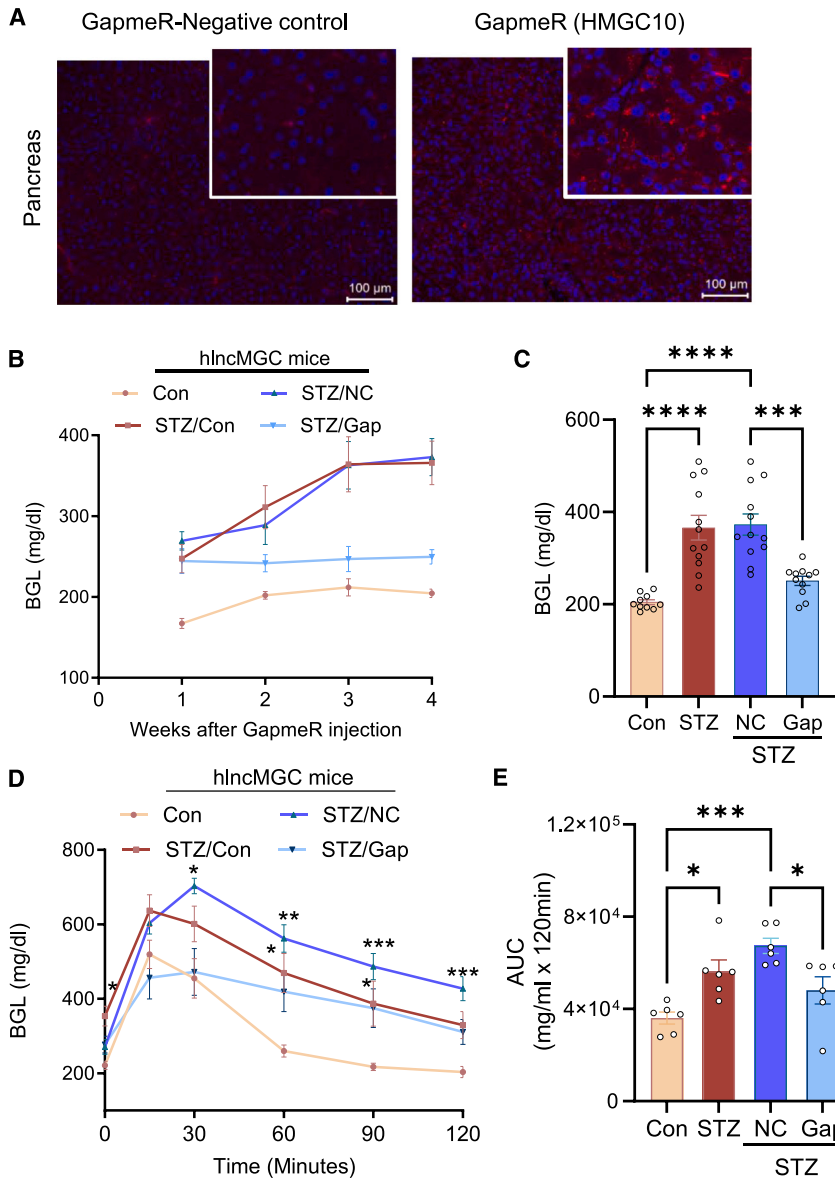
A GapmeR-targeting lncMGC increases insulin-positive cells in STZ mice

A GapmeR-targeting lncMGC accumulated in mouse kidneys and alleviated key features of kidney damage in T1D mice.[17] Extending this, mice treated with the GapmeR (5 mg/kg) targeting lncMGC (MGC10) showed *in situ* hybridization pancreatic accumulation of the oligonucleotide (Figure S2A). Insulin-positive cells were decreased in islets from STZ (50 mg/kg/day, for 5 consecutive days) and STZ/GapmeR-negative control (NC) mice, but significantly increased in islets after treatment with the lncMGC-targeting GapmeR (5 mg/kg/week for 4 weeks) (Figures S2B and S2C).

A GapmeR-targeting hlncMGC prevents T1D in hlncMGC mice

lncMGC sequences are not 100% conserved from mouse to human. The conservation between mouse and hlncMGC is 88% at the level

A GapmeR-Negative control | GapmeR (HMGC10)

Pancreas

100 μm | 100 μm

B hlncMGC mice

BGL (mg/dl)

Con | STZ/NC
STZ/Con | STZ/Gap

Weeks after GapmeR injection

C

****

**** ***

BGL (mg/dl)

Con STZ NC Gap
STZ

D hlncMGC mice

BGL (mg/dl)

Con | STZ/NC
STZ/Con | STZ/Gap

Time (Minutes)

E

***

* *

AUC (mg/ml × 120min)

Con STZ NC Gap
STZ

Figure 3. GapmeR-targeting hlncMGC (HMGC10) prevents the development of diabetes in hlncMGC mice

(A) Representative images show accumulation of GapmeR (HMGC10) in pancreas tissue using *in situ* hybridization with a fluorescent antisense LNA-modified probe. hlncMGC mice were injected with GapmeR-NC or with GapmeR (HMGC10)-targeting hlncMGC 5 mg/kg weekly for 4 weeks. Scale bar, 100 μm. 20× magnification. (B) Diabetes was induced by injecting 10-week-old hlncMGC male mice with 40 mg/kg STZ or vehicle Con (citrate buffer) intraperitoneally daily for 4 consecutive days. (B and C) Weekly (B) and (C) endpoint BGLs in 4 groups of hlncMGC mice: Con, diabetic (STZ/Con), diabetic mice injected with GapmeR-NC (STZ/NC), and diabetic mice injected with GapmeR (HMGC10) (STZ/Gap) 5 mg/kg weekly for 4 weeks. GapmeR was injected after onset of diabetes. n = 10–12 mice/group. (D) GTT. *p < 0.05; **p < 0.01; ***p < 0.001; STZ/Con and STZ/NC versus Con using 2-way repeated-measures ANOVA. n = 6–7 mice/group. (E) AUC at 4 weeks of diabetes. One-way ANOVA with post hoc Tukey's test for multiple comparisons. *p < 0.05; ***p < 0.001; ****p < 0.0001. Data are presented as mean ± SEM.

(*Bcl2*) and mitochondrial (*Fis1*)[23] mRNAs were increased, but pro-apoptosis associated mRNAs (*Puma*, *Bad*, *Bid*, *Bim*)[26] were decreased (Figure 5C). These results are consistent with findings in lncMGC KO mice (see Figures 2A and 2E).

A GapmeR-targeting lncMGC prevents hyperglycemia and insulitis in NOD mice

NOD mice show islet inflammation and, with aging, tend to develop diabetes, which is more consistent in female mice.[30] Female NOD mice (8-week-old) received the GapmeR-NC or the GapmeR-targeting lncMGC (MGC10) (5 mg/kg weekly for 7 weeks) before the onset of hyperglycemia (Figure 6)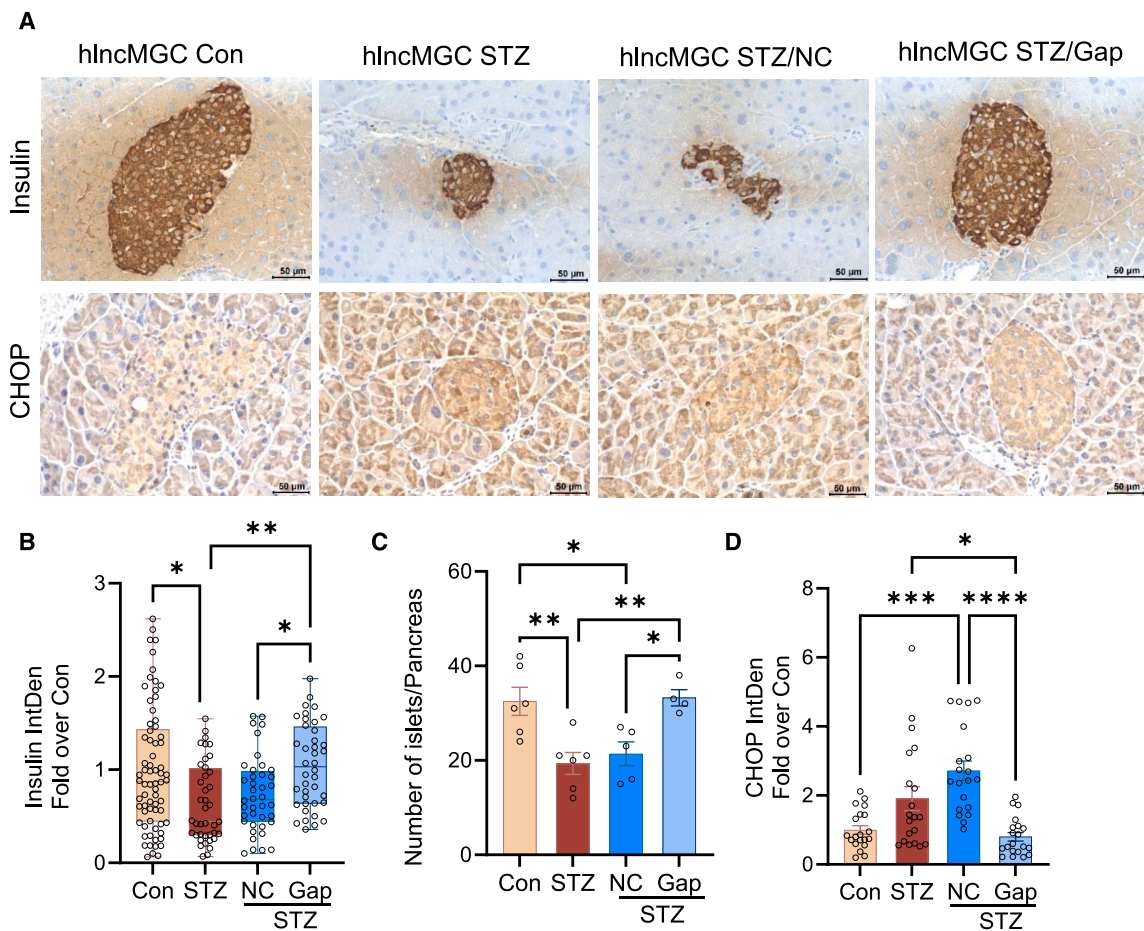. BGLs were decreased in GapmeR-injected NOD mice (NOD/Gap) compared to NOD/NC mice (Figures 6A and 6B). Immunofluorescence (IF) staining of CD3 (a marker of T cells) showed more immune cell infiltration (green) in the islets from NOD and NOD/NC mice compared to the Con Scid mice (Figure 6C). Scid mice have immune aberrations and do not show insulitis and diabetes.[31] Interestingly, the lncMGC GapmeR reduced the percentage of severe insulitis in NOD/Gap mice (Figures 6C and 6E). Insulitis levels were scored as no insulitis (0% immune cell infiltration), peri- (<25%), moderate (25–75%), and severe (>75%)[32] (Figures 6D and 6E). CHOP, the ER stress marker, was increased in islets from NOD and NOD/NC mice compared to Con (NOD/Scid) mice, whereas this increase was clearly attenuated in islets from NOD/Gap mice (Figures 6C and 6F).

CHOP levels were attenuated in islets from GapmeR-treated hlncMGC STZ mice (Figures 4A and 4D).

GapmeR treatment increases viability of isolated islets from hlncMGC mice

Islets from hlncMGC mice were treated with the targeting or Con GapmeR using Gymnosis.[29] After treatment, vital dyes were used to stain mouse islets. Fluorescein diacetate (FDA, green) marks viable cells and propidium iodine (PI, red) marks dead cells (Figure 5A). Treatment with the hlncMGC targeting GapmeR (HMGC10, 1 μM) increased islet viability (Figures 5A and 5B) and corresponded to a reduction in lncMGC RNA (Figure 5C). miR-379 was also lower in GapmeR-treated islets (Figure 5C). Notably, after GapmeR treatment, anti-ER stress (*Edem3*, target of miR-379)[17,25] and anti-apoptotic

Figure 4. Pancreas structure, insulin levels, and key functional markers in GapmeR-treated hlncMGC STZ diabetic mice

(A) IHC staining of insulin and CHOP in pancreatic islets of hlncMGC Con, diabetic (STZ/Con), diabetic mice injected with GapmeR-NC (STZ/NC), and STZ mice injected with GapmeR (HMGC10) (STZ/Gap) 5 mg/kg weekly for 4 weeks. Scale bar, 50 μm. 40× magnification. (B and C) Quantitative analysis of (B) insulin ($n = 70$ islets/Con group and $n = 40$ islets/STZ, STZ/NC, STZ/Gap groups) and (C) number of pancreatic islets in each group. (D) Quantitative analysis of CHOP ($n = 20$ islets/group). IntDen, 4 weeks after onset of diabetes. Kruskal-Wallis test with Dunn's multiple comparisons test. $*p < 0.05$; $**p < 0.01$; $***p < 0.001$; $****p < 0.0001$. Data are presented as mean ± SEM.
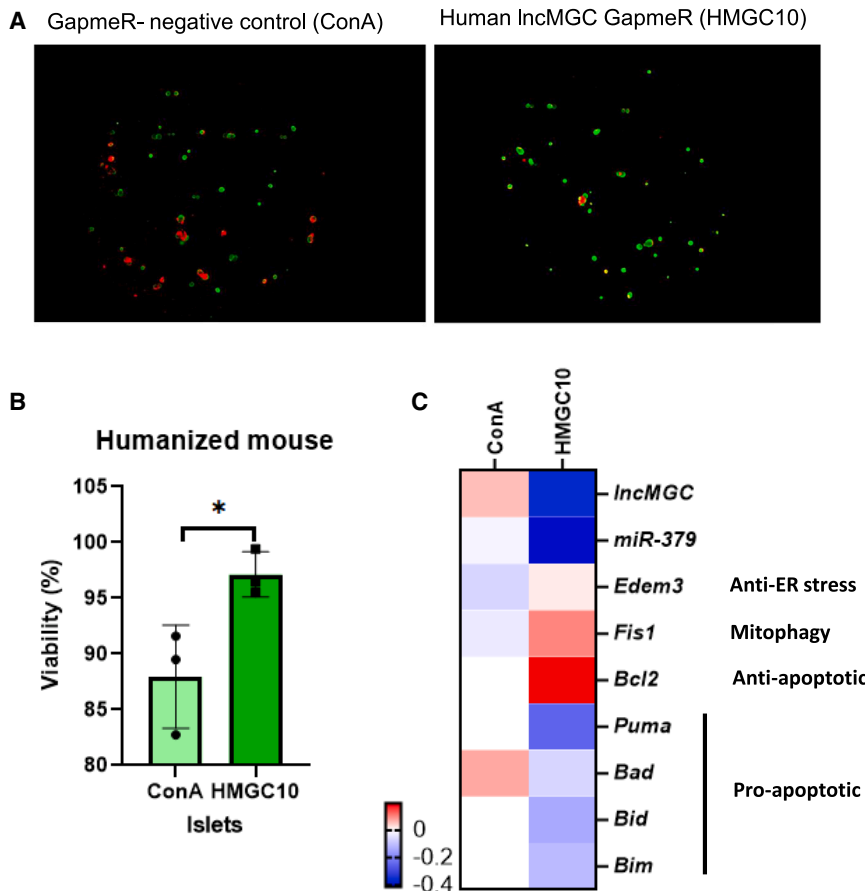
GapmeR-targeting lncMGC decreases hyperglycemia in diabetic Akita mice

Akita mice have a mutation in the *Ins2* gene (Cys96Tyr) that results in misfolding of an insulin precursor and ER stress in β cells and diabetes development.[33,34] Akita male mice (10 weeks old) were treated with GapmeR-NC or GapmeR-targeting lncMGC (GapmeR) (5 mg/kg weekly for 4 weeks) (Figure 7). BGLs were partially normalized in Akita/Gap mice and relatively lower compared to Akita or Akita/NC mice. (Figure 7B). Pancreata from Akita/Gap mice exhibited larger islets and increased insulin compared to Akita and Akita/NC mice (Figures 7A–7D). CHOP expression was lower in Akita/Gap islets compared to Akita/NC islets (Figures 7A and 7E). Related to this, we recently showed that ER stress was reduced in diabetic[23] and obese miR-379 KO mice.[24,35] Given these observations, we crossed Akita mice with miR-379KO mice (Figure S5A). Akita/miR-379KO male and female mice (3 weeks old) had lower BGLs compared to Akita mice (Figures S6A and S6B). Insulin-pos- itive islets were more frequent (Figures S6C–S6E), and CHOP was significantly lower in Akita/miR-379KO than in Akita mice (Figures S6C, S6F, and S6G). Similar observations were reported in Akita/CHOP-KO mice.[34] These results bolster the idea that lowering lncMGC lessens ER stress.

A GapmeR-targeting hlncMGC supports viability of isolated human islets

Islets from individuals with T1D are quite rare and not easy to obtain. This being the case, we were able to obtain islets from in- dividuals with type 2 diabetes (T2D) which showed higher levels of both lncMGC and miR-379 versus islets from non-diabetic indi- viduals (Figure 8A; Table S1). Islets from four non-diabetic donors were more viable after treatment with GapmeR-targeting hlncMGC (HMGC10 1 μM for 4 days) (Figures 8B–8D). Similar improve- ment in viability was also observed in GapmeR-treated islets from individuals with T2D (Figures 8E and 8F). Notably, the

A GapmeR- negative control (ConA)   Human lncMGC GapmeR (HMGC10)

B

C

Anti-ER stress

Mitophagy

Anti-apoptotic

Pro-apoptotic

Figure 5. GapmeR-targeting hlncMGC significantly increases viability in isolated islets from hlncMGC mice

(A) Isolated islets from hlncMGC mice were treated with a GapmeR-NC (ConA) and GapmeR (HMGC10) 1 µM for 4 days and stained with 0.48 µM FDA to show viable cells (green) and 10 µg/mL PI to show dead cells (red). (B) Viability of islets was calculated based on the total viable cell area relative to the total islet area (viable and dead) in the micrograph image. (C) Heatmap shows the expression of lncMGC, miR-379, *Edem3* (an anti-ER stress marker and a target of miR-379), *Bcl2* (anti-apoptotic), *Fis1* (mitophagy marker and a target of miR-379), and *Puma*, *Bad*, *Bid*, *Bim* (pro-apoptotic genes) in ConA and HMGC10-treated islets. *$p < 0.05$. Statistical comparisons between 2 groups were performed using 2-sided Student's t tests. Data are presented as mean ± SEM.

hlncMGC targeting GapmeR HMGC10 decreased the levels of both lncMGC and miR-379 in human islets (Figure 8G). In parallel, the expression of pro-apoptotic genes (*PUMA*, *BIM*, and *BID*) as well as hlncMGC and miR-379 was decreased, while the expressions of anti-apoptotic gene (*BCL2*) and anti-ER stress gene (*EDEM3*) were increased in human islets treated with HMGC10 GapmeR (Figure 8G). Pro-inflammatory cytokines induce human islet death.[36] Interestingly, GapmeR-treated islets from a non-diabetic individual showed resistance to pro-inflammatory cytokine-driven cell death (Figure 8H). In addition, the expressions of lncMGC, miR-379, and HSPA5 (an ER stress maker)[37] were increased in these human islets treated with cytokines and decreased by the GapmeR HMGC10 targeting hlncMGC (Figure 8I), suggesting that lncMGC and miR-379 are upregulated by ER stress induced by cytokine treatment. These results are summarized schematically in Figure 8J.

DISCUSSION

Here, we report that correction and prevention of diabetes were observed in STZ-injected lncMGC KO mice as well as GapmeR-targeting lncMGC-treated NOD, Akita, and partially hlncMGC-STZ mice. ER stress factor CHOP was increased in islets from diabetic mice but attenuated in lncMGC KO mice and mice treated with the GapmeR-targeting lncMGC. The expressions of anti-ER stress (*Edem3*, a target of miR-379) and anti-apoptotic (*Bcl2*) genes were increased, but pro-apoptotic (*Puma*, *Bad*, *Bid*, *Bim*) genes were decreased in lncMGC KO islets and GapmeR-treated islets. Since ER stress induces cell death through Bcl2 family factors related to apoptosis,[38] lowering lncMGC, ER stress, and pro-apoptotic gene activity can protect pancreatic β cells. Because ER stress is associated with T1D,[39] lowering lncMGC and associated ER stress and pro-apoptotic gene activity can protect pancreatic β cells and reduce diabetes development.

A GapmeR-targeting hlncMGC lowered BGLs in STZ-injected hlncMGC mice. The hlncMGC was elevated in islets from T2D patients compared to Con non-diabetic subjects. A GapmeR-targeting hlncMGC increased the viability of islets from both healthy and T2D donors. We were unable to procure islets from T1D subjects due to limited availability. Similar to that in mouse islets, the expressions of *EDEM3* and *BCL2* were increased but pro-apoptotic (*PUMA*, *BAD*, *BID*, *BIM*) genes were reduced in human islets treated with the GapmeR. Of note, *PUMA* is a marker for human islet damage.[26] We previously showed that the lncMGC GapmeR inhibits expression of the miR-379 cluster and features of early DKD in mice through reduction in ER stress.[17] In the present study, inhibition of lncMGC may protect pancreatic islets through similar (ER stress-related) mechanisms found in kidney protection but also slightly different mechanisms (Bcl2 family-related cell death and others). Overall, our current data suggests the lncMGC/miR-379/EDEM3/ER stress/BCL2 family axis is a valuable target for the prevention of T1D (Figure 8J).

Diabetic Akita mice have a mutation in the *ins2* gene (Cys96Tyr) that affects the proper folding of insulin peptides.[33,34] Onset of diabetes
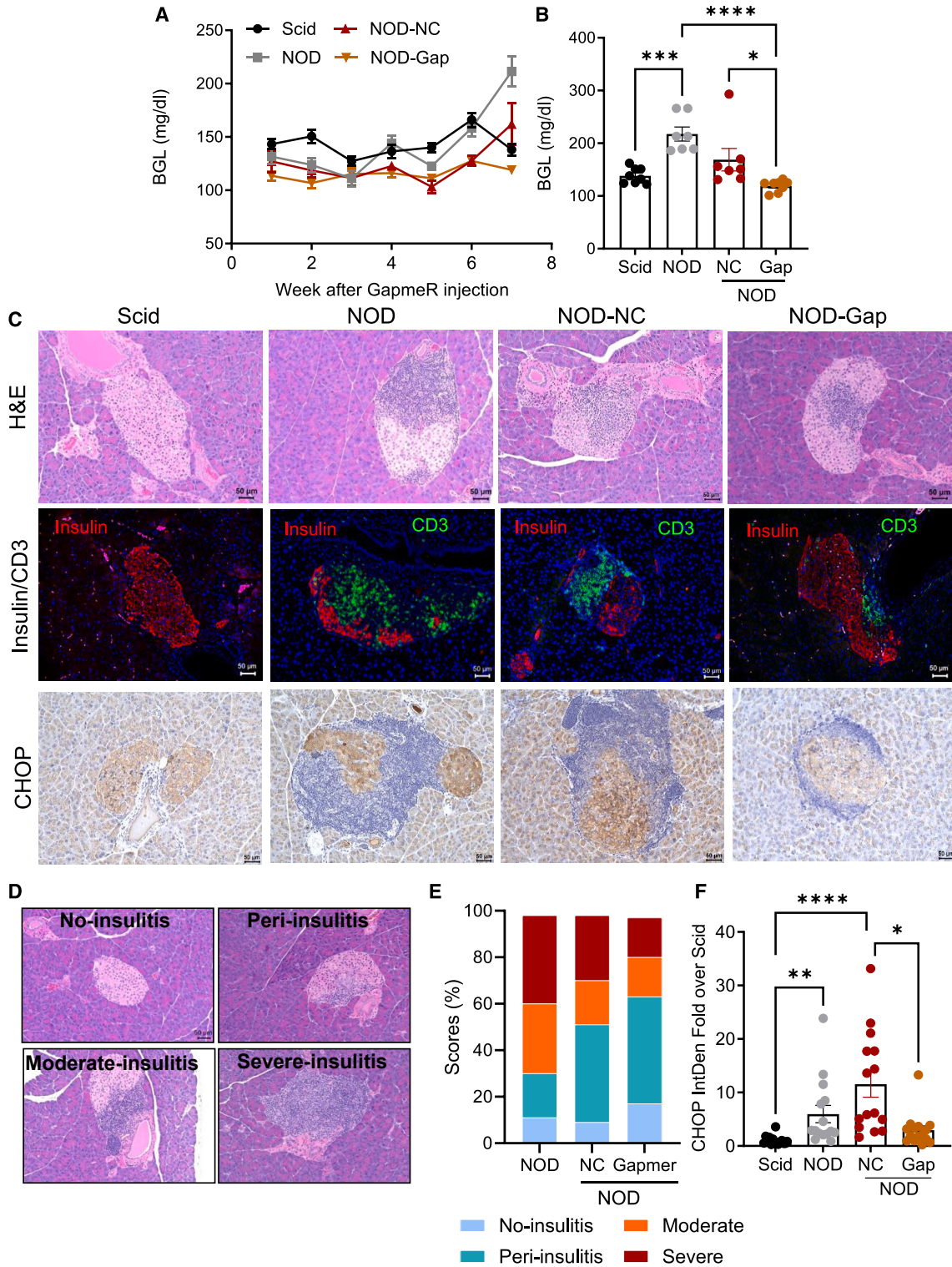
Figure 6. GapmeR-targeting lncMGC prevents hyperglycemia and insulitis in NOD female mice

(A and B) Weekly (A) and (B) endpoint BGLs in Con Scid, female diabetes-prone NOD mice (NOD), and NOD mice injected with GapmeR-NC (NOD/NC) or NOD mice injected with GapmeR (MGC10) (NOD/Gap) (5 mg/kg weekly for 7 weeks). n = 7–8 mice/group. (C) Top: H&E-stained pancreatic tissue sections from respective mice. Center: IF

(legend continued on next page)

was delayed in Akita/CHOP-KO mice compared to Akita mice,[34] suggesting that misfolded insulin peptide may cause ER stress mediated by CHOP. In the present study, we also observed protection from diabetes in Akita mice treated with GapmeR-targeting lncMGC and when crossed with miR-379KO mice. Again, these observations further confirm that CHOP-driven ER stress and lncMGC are critical factors for the pathogenesis of diabetes, and that miR-379 is one of the key effectors of lncMGC.

Notably, lncMGC as well as miR-379 were increased in human islets from individuals with T2D relative to Con subjects. Interestingly, islet viability was improved after exposure to the GapmeR-targeting hlncMGC. Dysfunction of β cells has been reported in T2D and insulin resistance.[40,41] These novel data imply that increased lncMGC may play a role in the pathogenesis of not only T1D but also T2D, and inhibition of lncMGC may also be effective in preventing T2D with potential broader therapeutic implications. However, further studies in mouse models of T2D are needed to investigate this.

Our data suggest that the effects of lncMGC are both miR-379 dependent and miR-379 independent. EDEM3 (ER stress related) and FIS1 (mitophagy related) are known targets of miR-379, as we reported.[23] Anti-apoptotic gene BCL2 is a potential target of miR-379 and reduced by miR-379 in lung cancer.[42] Therefore, the alterations of these ER stress, mitophagy, and anti-apoptotic genes by the lncMGC GapmeR treatment can be explained as targets of miR-379. lncMGC RNA promotes chromatin opening at target loci by interacting with nucleosome remodelers such as SMARCA5 and enhance the DKD-related gene expression and lncMGC itself. The SMARCA5/lncMGC complex opens the chromatin at target gene loci through zinc finger and AT-rich sites in the promoter of lncMGC.[18] Smarca5 small interfering RNA reduced the expression of lncMGC, miR-379, and DKD-related genes.[18] These DKD-related genes are not direct targets of miR-379. The expression of lncMGC, miR-379, and DKD-related genes and SMARCA5 enrichment at the promoter of lncMGC were reduced in lncMGC-KO kidney cells,[18] also implicating regulation of its own promoter by lncMGC and SMARCA5. Therefore, lncMGC upregulates its own promoter by interacting with SMARCA5 and thereby enhances the expression of lncMGC, miR-379, and other downstream disease-related genes, and these events are ameliorated by KO or knockdown of lncMGC via lncMGC/SMARCA5-mediated mechanisms. However, EDEM3, FIS1, and BCL2 are targeted by miR-379 but not regulated by lncMGC/SMARCA5-mediated mechanisms. Thus, KO or knockdown of lncMGC in pancreatic cells can also upregulate miR-379 targets EDEM3, FIS1, and BCL2 indirectly due to miR-379 reduction.

Autoimmunity is known to initiate T1D.[2,7] Highly accumulated misfolded or unfolded insulin peptides in Akita mice islet β cells can serve as autoantigens for islet T cells, which might cause autoimmune T1D in these mice. NOD mice display an autoimmune form of diabetes. We found that lncMGC GapmeR-treated NOD mice had less hyperglycemia and insulitis. These results suggest that lncMGC may also be involved in autoimmune T1D perhaps via ER stress induced by unfolded insulin peptides, which can be autoantigens. We previously screened lncMGC RNA-interacting proteins by mass spectrometry and identified several RNA-binding proteins such as IQGAP, SMARCA5, SMARCC2, DBC1, BAT2, and YBX1.[18] Nucleosome remodelers such as SMARCA5 and SMARCC2 are also identified as proteins binding to an lncRNA, lncTCF7, suggesting involvement of lncMGC in cell renewal, stemness, and transdifferentiation through Wnt signaling, which are implicated in lncTCF actions.[43,44] More interesting is that some of these RNA-binding proteins are also related to autoantigens in autoimmune diseases, including diabetes.[45,46] IQGAP was suggested to be involved in T cell activation (NFAT) through interacting with lncRNA NRON.[47,48] These observations suggest that besides reductions in miR-379, there are likely additional mechanisms by which lowering lncMGC may ameliorate diabetes in mice and support islet viability. It may be worth examining whether lncMGC binding protein interactions foster autoimmune diabetes.

As mentioned above, miR-379 is one of the major downstream lncMGC effectors targeting EDEM3,[17] FIS1,[23] and potentially BCL2[42] because lncMGC is a hosting noncoding RNA for a miRNA cluster that includes miR-379.[17] In fact, we found that Akita/miR-379KO mice were protected from hyperglycemia compared to Akita mice. However, other miRNAs such as miR-494 (targeting ATF3 inhibiting CHOP) are also regulated by lncMGC, and may also act as effectors of lncMGC.[17] As discussed above, lncMGC RNA also has miR-379-independent actions/functions (associated with chromatin remodeling and auto-immunity). These observations suggest miR-379 is not the only downstream effector of lncMGC related to autoimmune T1D development. Therefore, targeting lncMGC is slightly different from targeting the single miRNA miR-379, although miR-379 could be a major effector. Targeting lncMGC may have additional beneficial effects for T1D treatment than targeting only miR-379.

In the present study, we used global lncMGC KO or humanized mice. GapmeR-targeting lncMGC can accumulate in other tissues, including liver and kidney.[17] Therefore, the effects of lncMGC KO or GapmeR in other tissues besides the islets may contribute to the observed protective phenotypes. It is well known that pancreatic β cells are the major targets in STZ-induced T1D because, due to the similarity of the structures of STZ and glucose, STZ is preferentially uptaken by β cells through the GLUT2 glucose transporter, which

staining for insulin (red) and CD3 (green). Bottom: IHC staining for CHOP. (D) Using H&E sections, images of islets were scored based as shown (representatively) on the percentage of area of insulitis/islet: no (0% immune cell infiltration), peri- (<25%), moderate (25%–75%), and severe (>75%). (E) Severe insulitis was reduced by GapmeR injection in NOD mice. (F) Quantitative analysis of CHOP (n = 15 islet/group). Scale bar, 50 μm. 20× magnification. One-way ANOVA with post hoc Tukey's test for multiple comparisons. *p < 0.05; **p < 0.001; ***p < 0.001; ****p < 0.0001. Data are presented as mean ± SEM.
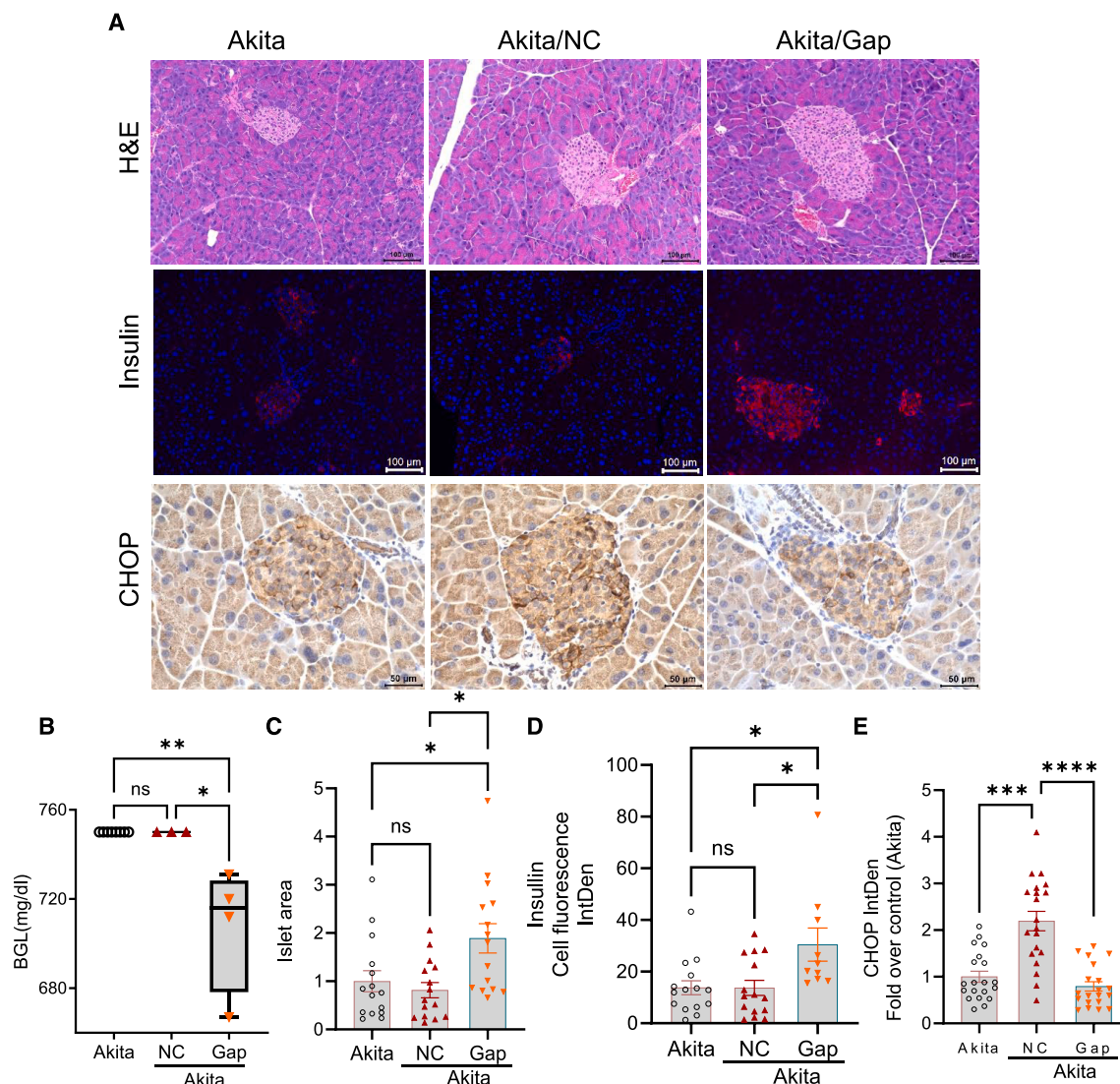
Figure 7. GapmeR-targeting lncMGC prevents hyperglycemia in male Akita mice

(A) Top: H&E representative images for histology of pancreas in Akita Con (Akita), Akita mice injected with GapmeR-NC (Akita/NC), and Akita mice injected with GapmeR (MGC10) (Akita/Gap) 5 mg/kg weekly for 4 weeks. Center: IF staining for insulin (red signals). Scale bar, 100 μm. 20× magnification. Bottom: IHC staining for CHOP. Scale bar, 50 μm. 40× magnification. (B) Endpoint BGL ($n = 8$/Akita, $n = 3$/Akita/NC, and $n = 4$/Akita/Gap). (C) Pancreatic islet size was measured using ImageJ ($n = 15$ islets/group). (D and E) Quantification of insulin intensity ($n = 10–14$ islets/group) (D) and (E) CHOP levels ($n = 20$ islets/group). Kruskal-Wallis test with Dunn's multiple comparisons test. $*p < 0.05$; $**p < 0.001$; $***p < 0.001$; $****p < 0.0001$; ns, not statistically significant. Data are presented as mean ± SEM.

is mainly present in β cells.[49] Since STZ is identified as a DNA-damaging agent, it preferentially kills β cells, although STZ may have some toxic effects in other tissues such as kidney and liver. However, STZ-induced injury of pancreatic β cells with subsequent loss of insulin is the major mechanism for hyperglycemia and the insulin-deficient T1D phenotype. As shown in Figure 4, STZ led to a reduced number and size of the mouse islets, and these were ameliorated by treatment with the lncMGC GapmeR. To our knowledge, the STZ-induced T1D phenotype, including hyperglycemia and loss of insulin, is primarily due to islet injury and β cell death.[49] In our study, the

observed protections from STZ-induced hyperglycemia in the global lncMGC KO- and lncMGC GapmeR-treated hlncMGC mice are most likely due to the protective effects of lowering lncMGC in pancreatic β cells, although other mechanisms cannot be ruled out completely.

Taken together, lowering lncMGC, either in lncMGC KO mice or via GapmeR treatments, ameliorated T1D and increased the viability of mouse and human islets. This was, in part, likely via limiting ER stress. EDEM3 (ER stress), Bcl2 family (cell death), Fis1 (mitophagy), and RNA-binding proteins add another layer to the mechanism.
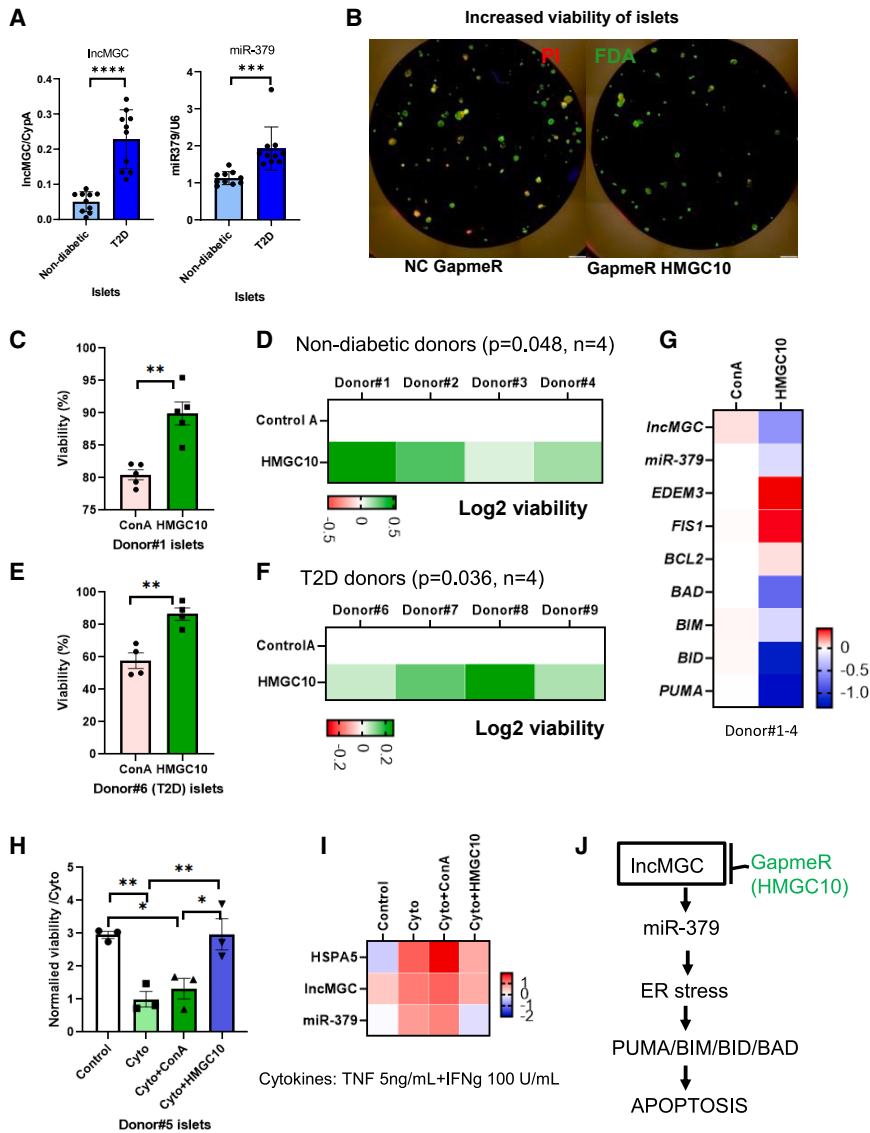
Figure 8. GapmeR HMGC10-targeting hlncMGC increases human islet viability

(A) lncMGC and miR-379 expression in isolated islets from individuals with and without T2D. (B) Representative data showing viability of human islets from non-diabetic individuals assessed using FDA/PI staining after GapmeR treatment (1 μM GapmeR HMGC10-targeting hlncMGC or GapmeR-NC (ConA) for 4 days). Green (FDA) shows viable cells and red (PI) shows dead cells. (C) Viability of GapmeR (HMGC10)-treated islets compared to GapmeR-NC (ConA) from a non-diabetic donor. (D) Data from islets from 4 non-diabetic donors (Donor#1–#4) show they are more viable after HMGC10 treatment (1 μM for 4 days). (E and F) Viability in GapmeR-treated islets from individuals with T2D (Donor#6–9). (G) Expression of *hlncMGC*, *miR-379*, *EDEM3*, *PUMA*, *BIM*, and *BID* (pro-apoptotic genes) and *BCL2* (anti-apoptotic gene) in human islets treated with HMGC10 GapmeR versus NC. (H) Viability of human islets from a non-diabetic individual (Donor#5) after pro-inflammatory cytokine mixture (5 ng/mL TNF-α and 100 U/mL interferon-γ) plus GapmeR treatment (Cyto + HMGC10) compared to NC (Cyto + ConA). (I) Expression of *hlncMGC*, *miR-379*, and *HSPA5* in non-diabetic individual (Donor#5) after pro-inflammatory cytokine mixture plus GapmeR treatment. (J) In diabetes, ER stress results in increased expression of lncMGC (and miR-379), which further increases ER stress and expression of apoptotic genes fostering β cell death while the GapmeR-targeting hlncMGC inhibits these adverse events and protects islets from apoptosis.

A GapmeR-targeting hlncMGC deserves consideration as an approach to intersect and limit or correct diabetes.

MATERIALS AND METHODS

Generation of partially hlncMGC mice

All animal studies were conducted according to protocols approved by the Institutional Animal Care and Use Committee at the Beckman Research Institute of City of Hope National Medical Center. lncMGC KO mice were created as described.[18] The conservation between mouse and hlncMGC is 88% at the level of nucleotide sequence.[17] The GapmeR target site has a mismatch between mouse and human sequences, which is the major reason this site was chosen for replacing the mouse lncMGC with hlncMGC (to make partially hlncMGC mice), so the resulting mouse-human hybrid sequence can be targeted by the hlncMGC targeting GapmeR. To create partially hlncMGC mice, CRISPR guide RNA design software (CRISPR direct) was used to choose the single-guide RNAs (sgRNAs) targeting lncMGC as described.[18,50] A mixture of two CRISPR sgRNAs flanking the transcription start site of lncMGC (5′-GAGUUAGU GUGGCCUUCAUC-3′ and 5′-GCACGGUG CUGAAAGAGAGG-3′ (Synthego) (50 ng/μL total), single-strand mouse-human chimeric oligonucleotide (Megamer, IDT), 5′- ACTAGAGGTCTTTCA CATGGTGATCTATGCCATTGTGGTGTCCCCTTTATCTTGAT GAAGAGATAGTTGACCACATAATGGCCAAAGCATGGTCAG TATTGTACATTTTGCCTTGTCGCAGTCTTTCCAAGTTGACA TGGCCTTCCTGGAGGAATTACCACTTAGGGTAGAGGCACC CCTTCCCCCATCAATGCCACTGCCCCACATTGGAGGAGGG GTTGTTTATGTTCACCATGTGCCTG*CTTCCAATGCCAAATC* CAGCCTCAGAAAGCTTTCTGGAAGTGACGCCAACTTCAGG GGCAAGGCCCTGGTTCTGGGGTCAGCACCATTCCGTGGTT CCTGAAGAGATGGTAGACTATGGAACGTAGGCGTTATGAT TTCTGACCTATGTAACATGGTCCACTAACTCTCAGTATCCA ATCCATCCTCGGAGGGCACCCCGGAGGTGTTACCAACAGC GAGGAAGA-3′ (GapmeR target site in italic) and 50 ng/μL Cas9 enzyme (IDT) was microinjected into the pronuclei and cytoplasm of fertilized C57BL/6J embryos, as described previously.[51] The

microinjected embryos were implanted into pseudo-pregnant recipient female mice to produce mutant mice. Mice were screened using PCR of DNA from tail samples. Several mice had human sequence fragments that were confirmed by gene sequencing. Mutant mice were crossed with WT C57BL/6 mice and offspring tested for germline transmission of the hlncMGC. Heterozygotes were crossed to obtain homozygotes. Several mutant lines were obtained. The following PCR primers were used to separate the bands of mouse and human fragments in the agarose gel electrophoresis: mouse-specific forward primer 379upMF 5′-GTGATCTATGCCATTGTGGTGTC-3′, human-specific forward primer 379upHsF 5′-CCCTTTATC TTGATGAAGAGATAGTTGA-3′, and common reverse primer 379MHcommonR 5′-GGATACTGAGAGTTAGTGGACCATG-3′.

Mouse models of diabetes
As per the Diabetes Complications Consortium (https://www. diacomp.org/), diabetes was induced by injecting 10-week-old male mice with 50 or 40 mg/kg/day STZ intraperitoneally daily for 5 or 4 consecutive days. STZ (40 mg/kg/day for 4 days) was used as a relatively milder inducer of diabetes compared to 50 mg/kg/day for 5 days.[52] Male mice injected with citrate buffer served as Con. Diabetes was confirmed by measuring tail vein BGLs (non-fasting glucose >250 mg/dL). Unlike male mice, STZ-injected female mice of the same age did not develop high BGLs. Thus, female mice were not evaluated. NOD, NOD/Scid male mice, and Akita (Ins2$^{Akita+/-}$) male mice were obtained from The Jackson Laboratory and housed in pathogen-free conditions under a 12 h light/12 h dark cycle. We used NOD female mice because, unlike male mice, they start to develop diabetes earlier, between 10 and 14 weeks of age.[53] At the end of each experiment, the mice were humanely euthanized and tissues including plasma and pancreas were collected for further examination.

Metabolic assays
As a prelude to a glucose tolerance test (GTT), mice fasted for 5 h and then were given 2 g/kg glucose via intraperitoneal injection, and blood glucose was measured at 15, 30, 90, and 120 min. The BGL was monitored using a glucometer (Alpha Track), and the area under the curve (AUC) was calculated with GraphPad Prism software. HbA1c was measured in whole-blood samples using a HbA1c assay kit (no. 80310, Crystalchem), and the results were reported as %HbA1c.

Histology and IHC
The pancreata were removed, fixed with formalin, and embedded in paraffin. Deparaffinized tissue slides were prepared for H&E, IHC, and IF staining. For IHC, the following primary antibodies were used: anti-insulin (1:100, ab7842, Abcam) and anti-CHOP rabbit polyclonal antibody (1:100, 1524-1-AP, Proteintech). The secondary antibodies included goat anti-guinea pig (1:200, A18769, Invitrogen) and goat anti-rabbit (1:200, BA-1000, Invitrogen). For IF staining, the primary antibodies were anti-insulin (1:250, ab7842, Abcam) and anti-CD3 (1:250, ab5690, Abcam). The secondary antibodies were Alexa Fluor 647, goat anti-guinea pig immunoglobulin G antibody (1:400, A-21450, Invitrogen) and Alexa Fluor 488, goat anti-rabbit (1:400, A11034, Invitrogen). Images were taken at 20× magnification

(KEYENCE-BZ-800 series). Integrated density (IntDen) and fluorescence intensity were measured using ImageJ software (ImageJ.win32).

In situ hybridization
In situ hybridization was performed in the pancreas as described.[17,54] Paraffin pancreas slides were immersed in hybridization solution at 48°C for 30 min and then hybridized at 48°C for 5 min with a TEX615 Red (Exiqon) fluorescent-labeled LNA-modified oligonucleotide probe complementary to LNA-MGC10 followed by post-hybridization wash 3 times at 55°C in 0.1 × SSC. Slides were then stained with DAPI and images were taken at 20× magnifications using an IF microscope (KEYENCE-BZ-800) series).

GapmeRs
The GapmeRs used in this study were reported[17] : GapmeR-targeting mouse lncMGC, MGC10, ATTtggcagtgggAAG, uppercase: LNA; lowercase: DNA, full phosphorothioate (IDT). GapmeR-targeting hlncMGC, HMGC10, GATttggcattggAAG; uppercase: LNA; lowercase: DNA, full phosphorothioate. NC A, AACacgtctataCGC.

Human islets
Human islets were isolated by the Southern California Islet Cell Resource Center and distributed through the Arthur Riggs Diabetes & Metabolism Research Institute Translational Service Center at the City of Hope. The use of human islets in this study was granted by the institutional review board of the City of Hope (IRB protocol no. 01046). Table S1 provides information on donors of islets employed for RNA expression of lncMGC, and Table S2 provides information on islets used for *in vitro* viability assays. After isolation, islets were cultured in PIM-R culture medium (PRODO Laboratories) for 24 to 72 h at 37°C and 5% CO_2.

Mouse islet isolation
The mouse islets were isolated as reported.[55,56] Pancreata were infused with 2.5 mg/mL collagenase V (Sigma) dissolved in Hank's balanced salt solution and incubated at 37°C for 8 min. Tissue was then dissociated by vigorous shaking and washing several times. Islets were purified by Lymphocyte Separation Media (density 1.077 g/mL; Corning) centrifugation followed by hand picking.

Islet culture and viability assay
Islets (∼160 islet equivalents/well) were cultured in a 24-well suspension culture plate (Sarstedt) with 0.5-mL PIM-R culture medium containing 1 μM GapmeR-NC (Con A) or GapmeR-targeting hlncMGC (HMGC10) for 4 days. After the culture, islet viability was assessed by staining islets with 10 μg/mL PI (Millipore Sigma) and 0.48 μM FDA (Millipore Sigma). Images of islets were taken with an IXDP50 Olympus fluorescent microscope with a DP74 camera using a 4× objective lens (Olympus America). The viability (%) of each islet was determined as 100 − [area of PI/(area of FDA + PI) × 100] using cellSens software (Olympus America).[57] For some experiments, islets were cultured for 3 additional days with pro-inflammatory cytokines (5 ng/mL recombinant human tumor necrosis factor α [TNF-α] and 100 U/mL recombinant human interferon-γ; R&D Systems) before

viability analysis. To lessen the impact of heterogeneity among islet donors, the viability index was calculated by comparing the viability of islets treated with HMGC10 to the corresponding GapmeR-NC islets (Con A).

qRT-PCR

The qRT-PCR analysis was conducted as described.[23] RNA was extracted using the RNeasy Mini Kit (Qiagen). The mRNA expression data were normalized to *Cypa*, which served as an internal Con for mouse and human samples. Forward primers with specific mature miRNA sequences and the kit-provided universal primer were used for miRNA amplification (Quanta Biosciences). U6 served as the internal Con. Table S3 contains the sequences of primers employed.

Statistics and reproducibility

The statistical data analyses were conducted using GraphPad Prism software version 10.0.0. Prior to comparing between groups, the normal distribution of each sample group was confirmed using either the χ^2 test or the Shapiro-Wilk test. All data were presented as mean ± SEM, and statistical comparisons between two groups were performed using two-sided Student's t tests. For comparisons among multiple groups, ANOVA was applied, followed by the post hoc Tukey's test. Nonparametric tests (Kruskal-Wallis test with Dunn's multiple comparisons test) were performed for those data that failed normality and lognormality tests. The figure legends specify the number of replicates for each experiment. Significant differences are indicated by asterisks, with $*p < 0.05$, $**p < 0.01$, $***p < 0.001$, $****p < 0.0001$, and ns for not statistically significant.

DATA AND CODE AVAILABILITY

The data from this study are available from the authors upon request.

SUPPLEMENTAL INFORMATION

Supplemental information can be found online at https://doi.org/10.1016/j.omtn.2024.102252.

AUTHOR CONTRIBUTIONS

M.K., M.A., and R.N. designed the research. M.K., M.A., K.O., F.K., J.R., L.L., V.M., R.T., W.T., L.Z., and M.W. performed the research. M.K., M.A., and K.O. analyzed the data and generated all figures and tables. M.K., M.A., K.O., V.M., and R.N. wrote and edited the manuscript. All authors have read and approved the manuscript.

DECLARATION OF INTERESTS

M.K. and R.N. have an issued patent and pending patent applications through City of Hope disclosing and claiming certain parts of the work detailed in this paper. These pending applications and patents include the following two families: (1) US Patent Number 10,787,664, and US Patent Application No. 16/985,779 (published as U.S. Patent Application Publication No. 2020/0407721), which both claim priority to US Provisional Application No. 62/166,533; and (2) US Patent Application No. 17/268,068 (published as US Patent Application Publication No. 2021/0310000), which claims priority to PCT/US2019/046896 and US Provisional Application No. 62/719,566.

REFERENCES

1. Gan, M.J., Albanese-O'Neill, A., and Haller, M.J. (2012). Type 1 diabetes: current concepts in epidemiology, pathophysiology, clinical care, and research. Curr. Probl. Pediatr. Adolesc. Health Care *42*, 269–291.

2. Pugliese, A. (2017). Autoreactive T cells in type 1 diabetes. J. Clin. Invest. *127*, 2881–2891.

3. Eizirik, D.L., Cardozo, A.K., and Cnop, M. (2008). The Role for Endoplasmic Reticulum Stress in Diabetes Mellitus. Endocr. Rev. *29*, 42–61.

4. Tersey, S.A., Nishiki, Y., Templin, A.T., Cabrera, S.M., Stull, N.D., Colvin, S.C., Evans-Molina, C., Rickus, J.L., Maier, B., and Mirmira, R.G. (2012). Islet β-Cell Endoplasmic Reticulum Stress Precedes the Onset of Type 1 Diabetes in the Nonobese Diabetic Mouse Model. Diabetes *61*, 818–827.

5. Marhfour, I., Lopez, X.M., Lefkaditis, D., Salmon, I., Allagnat, F., Richardson, S.J., Morgan, N.G., and Eizirik, D.L. (2012). Expression of endoplasmic reticulum stress markers in the islets of patients with type 1 diabetes. Diabetologia *55*, 2417–2420.

6. Marselli, L., Thorne, J., Dahiya, S., Sgroi, D.C., Sharma, A., Bonner-Weir, S., Marchetti, P., and Weir, G.C. (2010). Gene expression profiles of Beta-cell enriched tissue obtained by laser capture microdissection from subjects with type 2 diabetes. PLoS One *5*, e11499.

7. Roep, B.O., and Peakman, M. (2012). Antigen targets of type 1 diabetes autoimmunity. Cold Spring Harb. Perspect. Med. *2*, a007781.

8. Hosoi, T., and Ozawa, K. (2009). Endoplasmic reticulum stress in disease: mechanisms and therapeutic opportunities. Clin. Sci. *118*, 19–29.

9. Shah, M.S., and Brownlee, M. (2016). Molecular and Cellular Mechanisms of Cardiovascular Disorders in Diabetes. Circ. Res. *118*, 1808–1829.

10. Kato, M., and Natarajan, R. (2019). Epigenetics and epigenomics in diabetic kidney disease and metabolic memory. Nat. Rev. Nephrol. *15*, 327–345.

11. Wang, L., Wang, H.L., Liu, T.T., and Lan, H.Y. (2021). TGF-Beta as a Master Regulator of Diabetic Nephropathy. Int. J. Mol. Sci. *22*, 7881.

12. Mattick, J.S., Amaral, P.P., Carninci, P., Carpenter, S., Chang, H.Y., Chen, L.-L., Chen, R., Dean, C., Dinger, M.E., Fitzgerald, K.A., et al. (2023). Long non-coding RNAs: definitions, functions, challenges and recommendations. Nat. Rev. Mol. Cell Biol. *24*, 430–447.

13. Font-Cunill, B., Arnes, L., Ferrer, J., Sussel, L., and Beucher, A. (2018). Long Noncoding RNAs as Local Regulators of Pancreatic Islet Transcription Factor Genes. Front. Genet. *9*, 524.

14. Arnes, L., and Sussel, L. (2015). Epigenetic modifications and long noncoding RNAs influence pancreas development and function. Trends Genet. *31*, 290–299.

15. López-Noriega, L., and Rutter, G.A. (2020). Long Non-Coding RNAs as Key Modulators of Pancreatic β-Cell Mass and Function. Front. Endocrinol. *11*, 610213.

16. Wallace, C., Smyth, D.J., Maisuria-Armer, M., Walker, N.M., Todd, J.A., and Clayton, D.G. (2010). The imprinted DLK1-MEG3 gene region on chromosome 14q32.2 alters susceptibility to type 1 diabetes. Nat. Genet. *42*, 68–71.

17. Kato, M., Wang, M., Chen, Z., Bhatt, K., Oh, H.J., Lanting, L., Deshpande, S., Jia, Y., Lai, J.Y.C., O'Connor, C.L., et al. (2016). An endoplasmic reticulum stress-regulated

lncRNA hosting a microRNA megacluster induces early features of diabetic nephropathy. Nat. Commun. 7, 12864.

18. Kato, M., Chen, Z., Das, S., Wu, X., Wang, J., Li, A., Chen, W., Tsark, W., Tunduguru, R., Lanting, L., et al. (2023). Long non-coding RNA lncMGC mediates the expression of TGF-β-induced genes in renal cells via nucleosome remodelers. Front. Mol. Biosci. 10, 1204124.

19. Charlier, C., Segers, K., Wagenaar, D., Karim, L., Berghmans, S., Jaillon, O., Shay, T., Weissenbach, J., Cockett, N., Gyapay, G., and Georges, M. (2001). Human-ovine comparative sequencing of a 250-kb imprinted domain encompassing the callipyge (clpg) locus and identification of six imprinted transcripts: DLK1, DAT, GTL2, PEG11, antiPEG11, and MEG8. Genome Res. 11, 850–862.

20. Hatada, I., Morita, S., Obata, Y., Sotomaru, Y., Shimoda, M., and Kono, T. (2001). Identification of a new imprinted gene, Rian, on mouse chromosome 12 by fluorescent differential display screening. J. Biochem. 130, 187–190.

21. Seitz, H., Royo, H., Bortolin, M.L., Lin, S.P., Ferguson-Smith, A.C., and Cavaillé, J. (2004). A large imprinted microRNA gene cluster at the mouse Dlk1-Gtl2 domain. Genome Res. 14, 1741–1748.

22. Zhang, J., Song, L., Ma, Y., Yin, Y., Liu, X., Luo, X., Sun, J., and Wang, L. (2020). lncRNA MEG8 Upregulates miR-770-5p Through Methylation and Promotes Cell Apoptosis in Diabetic Nephropathy. Diabet Metab Synd Ob 13, 2477–2483.

23. Kato, M., Abdollahi, M., Tunduguru, R., Tsark, W., Chen, Z., Wu, X., Wang, J., Chen, Z.B., Lin, F.M., Lanting, L., et al. (2021). miR-379 deletion ameliorates features of diabetic kidney disease by enhancing adaptive mitophagy via FIS1. Commun. Biol. 4, 30.

24. Abdollahi, M., Kato, M., Lanting, L., Wang, M., Tunduguru, R., and Natarajan, R. (2022). Role of miR-379 in high-fat diet-induced kidney injury and dysfunction. Am. J. Physiol. Ren. Physiol. 323, F686-f699.

25. Hirao, K., Natsuka, Y., Tamura, T., Wada, I., Morito, D., Natsuka, S., Romero, P., Sleno, B., Tremblay, L.O., Herscovics, A., et al. (2006). EDEM3, a Soluble EDEM Homolog, Enhances Glycoprotein Endoplasmic Reticulum-associated Degradation and Mannose Trimming. J. Biol. Chem. 281, 9650–9658.

26. Omori, K., Mitsuhashi, M., Ishiyama, K., Nair, I., Rawson, J., Todorov, I., Kandeel, F., and Mullen, Y. (2011). mRNA of the pro-apoptotic gene BBC3 serves as a molecular marker for TNF-α-induced islet damage in humans. Diabetologia 54, 2056–2066.

27. Chan, D.C. (2020). Mitochondrial Dynamics and Its Involvement in Disease. Annu. Rev. Pathol. 15, 235–259.

28. Youle, R.J., and van der Bliek, A.M. (2012). Mitochondrial fission, fusion, and stress. Science 337, 1062–1065.

29. Stein, C.A., Hansen, J.B., Lai, J., Wu, S., Voskresenskiy, A., Høg, A., Worm, J., Hedtjärn, M., Souleimanian, N., Miller, P., et al. (2010). Efficient gene silencing by delivery of locked nucleic acid antisense oligonucleotides, unassisted by transfection reagents. Nucleic Acids Res. 38, e3.

30. Aubin, A.M., Lombard-Vadnais, F., Collin, R., Aliesky, H.A., McLachlan, S.M., and Lesage, S. (2022). The NOD Mouse Beyond Autoimmune Diabetes. Front. Immunol. 13, 874769.

31. Vladutiu, A.O. (1993). The severe combined immunodeficient (SCID) mouse as a model for the study of autoimmune diseases. Clin. Exp. Immunol. 93, 1–8.

32. Pujol-Autonell, I., Ampudia, R.M., Monge, P., Lucas, A.M., Carrascal, J., Verdaguer, J., and Vives-Pi, M. (2013). Immunotherapy with Tolerogenic Dendritic Cells Alone or in Combination with Rapamycin Does Not Reverse Diabetes in NOD Mice. ISRN Endocrinol. 2013, 346987.

33. Wang, J., Takeuchi, T., Tanaka, S., Kubo, S.-K., Kayo, T., Lu, D., Takata, K., Koizumi, A., and Izumi, T. (1999). A mutation in the insulin 2 gene induces diabetes with severe pancreatic β-cell dysfunction in the Mody mouse. J. Clin. Invest. 103, 27–37.

34. Oyadomari, S., Koizumi, A., Takeda, K., Gotoh, T., Akira, S., Araki, E., and Mori, M. (2002). Targeted disruption of the Chop gene delays endoplasmic reticulum stress-mediated diabetes. J. Clin. Invest. 109, 525–532.

35. Abdollahi, M., Kato, M., Lanting, L., Tunduguru, R., Wang, M., Wang, Y., Fueger, P.T., Wang, Q., Huang, W., and Natarajan, R. (2022). miR-379 mediates insulin resistance and obesity through impaired angiogenesis and adipogenesis regulated by ER stress. Mol. Ther. Nucleic Acids 30, 115–130.

36. Kim, S., Kim, K.A., Suk, K., Kim, Y.H., Oh, S.H., Lee, M.K., Kim, K.W., and Lee, M.S. (2012). Apoptosis of human islet cells by cytokines. Immune Netw. 12, 113–117.

37. Laybutt, D.R., Preston, A.M., Åkerfeldt, M.C., Kench, J.G., Busch, A.K., Biankin, A.V., and Biden, T.J. (2007). Endoplasmic reticulum stress contributes to beta cell apoptosis in type 2 diabetes. Diabetologia 50, 752–763.

38. Szegezdi, E., Logue, S.E., Gorman, A.M., and Samali, A. (2006). Mediators of endoplasmic reticulum stress-induced apoptosis. EMBO Rep. 7, 880–885.

39. Meyerovich, K., Ortis, F., Allagnat, F., and Cardozo, A.K. (2016). Endoplasmic reticulum stress and the unfolded protein response in pancreatic islet inflammation. J. Mol. Endocrinol. 57. R1-r17.

40. Dludla, P.V., Mabhida, S.E., Ziqubu, K., Nkambule, B.B., Mazibuko-Mbeje, S.E., Hanser, S., Basson, A.K., Pheiffer, C., and Kengne, A.P. (2023). Pancreatic β-cell dysfunction in type 2 diabetes: Implications of inflammation and oxidative stress. World J. Diabetes 14, 130–146.

41. Cerf, M.E. (2013). Beta cell dysfunction and insulin resistance. Front. Endocrinol. 4, 37.

42. Jiang, Y., Zhu, P., Gao, Y., and Wang, A. (2020). miR-379-5p inhibits cell proliferation and promotes cell apoptosis in non-small cell lung cancer by targeting β-arrestin-1. Mol. Med. Rep. 22, 4499–4508.

43. Wang, Y., He, L., Du, Y., Zhu, P., Huang, G., Luo, J., Yan, X., Ye, B., Li, C., Xia, P., et al. (2015). The long noncoding RNA lncTCF7 promotes self-renewal of human liver cancer stem cells through activation of Wnt signaling. Cell Stem Cell 16, 413–425.

44. Tremblay, J.R., Lopez, K., and Ku, H.T. (2020). Correction: A GLIS3-CD133-WNT-signaling axis regulates the self-renewal of adult murine pancreatic progenitor-like cells in colonies and organoids. J. Biol. Chem. 295, 5175.

45. Liu, J., and Cao, X. (2023). RBP–RNA interactions in the control of autoimmunity and autoinflammation. Cell Res. 33, 97–115.

46. Kato, M., Wang, L., Putta, S., Wang, M., Yuan, H., Sun, G., Lanting, L., Todorov, I., Rossi, J.J., and Natarajan, R. (2010). Post-transcriptional up-regulation of Tsc-22 by Ybx1, a target of miR-216a, mediates TGF-{beta}-induced collagen expression in kidney cells. J. Biol. Chem. 285, 34004–34015.

47. Willingham, A.T., Orth, A.P., Batalov, S., Peters, E.C., Wen, B.G., Aza-Blanc, P., Hogenesch, J.B., and Schultz, P.G. (2005). A Strategy for Probing the Function of Noncoding RNAs Finds a Repressor of NFAT. Science 309, 1570–1573.

48. West, K.A., and Lagos, D. (2019). Long Non-Coding RNA Function in CD4(+) T Cells: What We Know and What Next? Noncoding. RNA 5, 43.

49. Eleazu, C.O., Eleazu, K.C., Chukwuma, S., and Essien, U.N. (2013). Review of the mechanism of cell death resulting from streptozotocin challenge in experimental animals, its practical use and potential risk to humans. J. Diabetes Metab. Disord. 12, 60.

50. Naito, Y., Hino, K., Bono, H., and Ui-Tei, K. (2015). CRISPRdirect: software for designing CRISPR/Cas guide RNA with reduced off-target sites. Bioinformatics 31, 1120–1123.

51. Quadros, R.M., Miura, H., Harms, D.W., Akatsuka, H., Sato, T., Aida, T., Redder, R., Richardson, G.P., Inagaki, Y., Sakai, D., et al. (2017). Easi-CRISPR: a robust method for one-step generation of mice carrying conditional and insertion alleles using long ssDNA donors and CRISPR ribonucleoproteins. Genome Biol. 18, 92.

52. Weide, L.G., and Lacy, P.E. (1991). Low-dose streptozocin-induced autoimmune diabetes in islet transplantation model. Diabetes 40, 1157–1162.

53. Chen, D., Thayer, T.C., Wen, L., and Wong, F.S. (2020). Mouse Models of Autoimmune Diabetes: The Nonobese Diabetic (NOD) Mouse. Methods Mol. Biol. 2128, 87–92.

54. Kato, M., Putta, S., Wang, M., Yuan, H., Lanting, L., Nair, I., Gunn, A., Nakagawa, Y., Shimano, H., Todorov, I., et al. (2009). TGF-beta activates Akt kinase through a microRNA-dependent amplifying circuit targeting PTEN. Nat. Cell Biol. 11, 881–889.

55. Ishiyama, K., Rawson, J., Omori, K., and Mullen, Y. (2011). Liver natural killer cells play a role in the destruction of islets after intraportal transplantation. Transplantation 91, 952–960.

56. Beilke, J.N., Kuhl, N.R., Van Kaer, L., and Gill, R.G. (2005). NK cells promote islet allograft tolerance via a perforin-dependent mechanism. Nat. Med. 11, 1059–1065.

57. Salgado, M., Gonzalez, N., Medrano, L., Rawson, J., Omori, K., Qi, M., Al-Abdullah, I., Kandeel, F., Mullen, Y., and Komatsu, H. (2020). Semi-Automated Assessment of Human Islet Viability Predicts Transplantation Outcomes in a Diabetic Mouse Model. Cell Transplant. 29, 963689720919444.